Contents lists available at ScienceDirect

# Nuclear Instruments and Methods in Physics Research A

# Quenching the scintillation in $CF_4$ Cherenkov gas radiator

T. Blake [f], C. D'Ambrosio [b], S. Easo [g,b], S. Eisenhardt [h], C. Fitzpatrick [c], R. Forty [b], C. Frei [b], V. Gibson [e], T. Gys [b], N. Harnew [j], P. Hunt [j], C.R. Jones [e], R.W. Lambert [d], C. Matteuzzi [a], F. Muheim [h], A. Papanestis [g,b,*], D.L. Perego [a,k,1], D. Piedigrossi [b], R. Plackett [i], A. Powell [j], S. Topp-Joergensen [j], O. Ullaland [b,k], D. Websdale [i], S.A. Wotton [e], K. Wyllie [b]

[a] Sezione INFN di Milano Bicocca, Milano, Italy
[b] European Organization for Nuclear Research (CERN), Geneva, Switzerland
[c] Ecole Polytechnique Fédérale de Lausanne (EPFL), Lausanne, Switzerland
[d] Nikhef National Institute for Subatomic Physics and VU University Amsterdam, Amsterdam, The Netherlands
[e] Cavendish Laboratory, University of Cambridge, Cambridge, United Kingdom
[f] Department of Physics, University of Warwick, Coventry, United Kingdom
[g] STFC Rutherford Appleton Laboratory, Didcot, United Kingdom
[h] School of Physics and Astronomy, University of Edinburgh, Edinburgh, United Kingdom
[i] Imperial College London, London, United Kingdom
[j] Department of Physics, University of Oxford, Oxford, United Kingdom
[k] Università di Milano Bicocca, Milano, Italy

## ARTICLE INFO

## ABSTRACT

$CF_4$ is used as a Cherenkov gas radiator in one of the Ring Imaging Cherenkov detectors at the LHCb experiment at the CERN Large Hadron Collider. $CF_4$ is well known to have a high scintillation photon yield in the near and far VUV, UV and in the visible wavelength range. A large flux of scintillation photons in our photon detection acceptance between 200 and 800 nm could compromise the particle identification efficiency. We will show that this scintillation photon emission system can be effectively quenched, consistent with radiationless transitions, with no significant impact on the photons resulting from Cherenkov radiation.

© 2015 CERN for the benefit of the Authors. Published by Elsevier B.V. This is an open access article under the CC BY license (http://creativecommons.org/licenses/by/4.0/).

## 1. Introduction

The LHCb experiment [1] is one of the four major experiments at the Large Hadron Collider, LHC, at CERN. The Ring Imaging Cherenkov, RICH, system [2] of the LHCb experiment consists of two RICH detectors that provide charged particle identification from 2 to 100 GeV/$c$. The RICH 2 detector is used to identify particles in the high momentum region 15–100 GeV/$c$. The RICH detectors use n-perfluorocarbon gases at room temperature and pressure as Cherenkov gas radiators: $C_4F_{10}$ is used in RICH 1 and $CF_4$ in RICH 2. Both gases were chosen for their low dispersion. A hybrid photon detector (HPD) has been developed in collaboration with industry specifically for application in the LHCb RICH system [3]. The HPDs employ vacuum tubes with a 75 mm active diameter. They have quartz entrance windows with a multialkali photocathode and encapsulated pixelated read-out. This has led to

a photon detector with very high single-photon detection efficiency coupled with extremely low electronic background noise. The RICH optical system as well as the photon detector is not sensitive below 200 nm.

$CF_4$ had been deemed unsuitable as Cherenkov radiator in other detectors due to the high scintillation yield, particularly for detectors where the photon detection used VUV-sensitive imaging devices based on CsI, TMAE or TEA [4]. Other studies showed similar results [5]. The estimated total scintillation photon yield per MeV of energy deposited in $CF_4$ was about 1200 photons/MeV $\times 4\pi$ [4]. About 75% of these photons were estimated to be emitted at wavelengths in the range 220–600 nm. The scintillation in $C_4F_{10}$ is, in comparison to $CF_4$, only a minor effect [5]. Our measurements, at room temperature and pressure [6], give a factor $\sim 40$ between the scintillation yields for the two gases (photons/MeV deposited) in our wavelength range. These results indicated that the $CF_4$ scintillation would not be a problem with a detection window above 200 nm; the distribution of scintillating photons is uniform whereas the optics of a Ring Imaging Cherenkov detector is inherently pointing. Simulation of the RICH detector geometry

and laboratory measurements of the $CF_4$ emission showed that the energy deposit per minimum ionizing particle would be 1.24 MeV with a scintillation yield of $\sim$1920 photons/MeV. The expected yield of detected photons was estimated assuming a charged particle multiplicity in RICH 2 $\sim$40 minimum ionizing particles. The number of detected scintillation photons would then be about 150, equivalent to introducing one additional photon hit on a Cherenkov ring image with $\sim$23 Cherenkov photon hits. The particle identification algorithm [7,8] is insensitive to unstructured background. The expectation, based on the above assumptions, was that the scintillation effect in RICH 2 would be detectable, but irrelevant for the particle identification efficiency.

## 2. Scintillation in the Cherenkov radiators

During the first half of 2010 it became evident that the charged particle multiplicity and hence the detector occupancy was larger than predicted. As the LHC luminosity increased a large and nearly uniform background over the photodetector plane was seen in RICH 2, which can be attributed to scintillation in $CF_4$ (the hit multiplicity distribution is shown in Fig. 1). No sign of this background was observed in RICH 1.

The background became unsustainable for data taking, due to the large event size and bandwidth limitations. A tolerable efficiency was restored with modifications to the FPGA firmware of the data acquisition board, the UKL1 [9]. It was however clear that this situation would become untenable as the beam luminosity increased.

With an LHC luminosity of $1 \times 10^{32}$ cm$^{-2}$ s$^{-1}$ the typical pixel hit multiplicity for proton–proton interactions containing a reconstructed $D^{*+} \rightarrow D^0 \pi^+$, with $D^0 \rightarrow K^- \pi^+$ decay is given in Table 1. This sample of events is chosen since the events are unbiased (in the sense that the RICH detectors are not involved in the selection of the sample). Furthermore, the topology of the D* events is such that almost all particles traverse both RICH 1 and RICH 2.

The expected multiplicities from simulation are also quoted. The simulation results are only weakly dependent on tracking and production cuts and do not include a simulation of scintillation in the RICH 2 detector. A large part of the difference between the number of pixel hits in data and simulation can be attributed to scintillation.

The distribution of hits in the RICH 2 detector as a function of the time delay between the proton–proton collision and the photon detector readout signal is shown in Fig. 2. The arrival time of the signal is modelled as a decaying exponential, convoluted
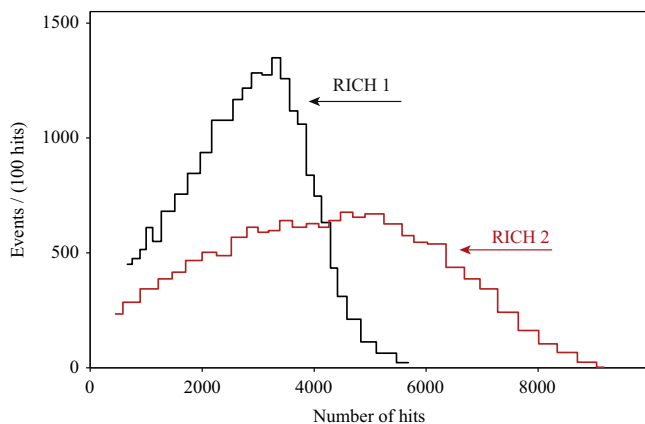
with a Gaussian to approximate the smearing due to the location of the HPD and the time-walk of the HPD readout. The effect of the delayed readout is to sweep a 25 ns window of integration time. The tail at large delay times is associated with scintillation light from the $CF_4$ radiator. The lifetime of the scintillation emission, estimated using this model, is about 10 ns.

Fig. 3 shows results from simulation of the time delay of HPD photoelectrons from three sources: Cherenkov radiation from the $CF_4$ gas, Cherenkov radiation from particles traversing the HPD quartz window and $CF_4$ scintillation. The quartz window contribution is not in fact a problem. Although the number of photoelectron hits is large they are concentrated in a few pixels, so they are suppressed by the binary readout which only records the presence

**Table 1**
Comparison between data and simulation conditions for proton–proton interactions containing a reconstructed $D^{*+} \rightarrow D^0 \pi^+$, with $D^0 \rightarrow K^- \pi^+$ decay. Most reconstructed tracks traverse both RICH 1 and RICH 2.

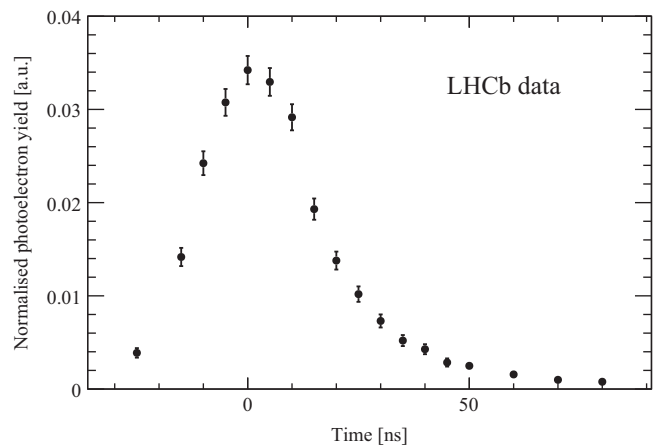|                     | p–p collision data | Simulation    |
| ------------------- | ------------------ | ------------- |
| Reconstructed tracks | $175.7 \pm 0.1$    | $158 \pm 1$   |
| RICH 1 hits         | $2321 \pm 1$       | $2361 \pm 15$ |
| RICH 2 hits         | $2342 \pm 1$       | $1588 \pm 11$ |



**Fig. 2.** Normalised photoelectron yield in the RICH 2 detector as a function of the time delay between the proton–proton collision and the photon detector readout signal. Total area is equal to one.
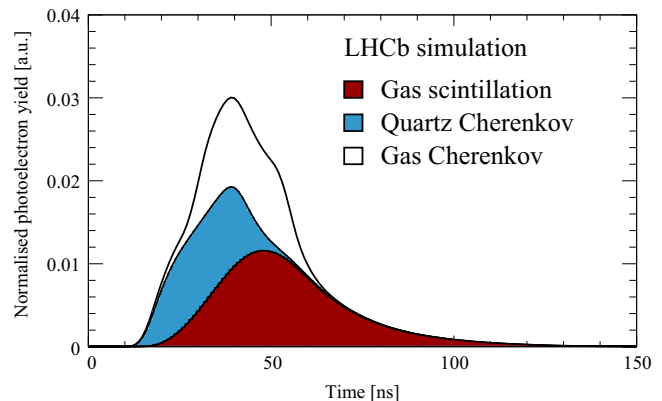


**Fig. 3.** Normalised photoelectron yield for simulated proton–proton collisions. Total area is equal to one. The contributions from Cherenkov light from the $CF_4$ radiator, Cherenkov light from the HPD quartz window and $CF_4$ scintillation are highlighted. Cherenkov emission from the quartz window results in large clusters of photo-electrons being produced in a single HPD. This signal is suppressed, with respect to the others, by the binary readout of the HPDs pixel sensor. The time offset between data, Fig. 2, and simulation is arbitrary.



**Fig. 1.** Histograms of the number of events as a function of the hit multiplicity observed in RICH 1 and in RICH 2. The bin width is (100 hits) and data were collected in 2010 with an LHC luminosity $\mathcal{L}$: $17.1 \times 10^{30}$ cm$^{-2}$ s$^{-1}$ and mean number of interactions per trigger, $\mu$: 2.05.

or absence of hits. Furthermore they are localised to the few ($< 1\%$) HPDs that are traversed by charged particles. These HPDs are easily recognised by the analysis software and their data excluded from the pattern recognition algorithm.

Further measurements were made to test for a long-lived component of the fluorescence, using calibration triggers to examine the activity in the RICH detectors during empty–empty bunch crossings at a delay of 300 ns after the last proton–proton collision. The number of hits observed in RICH 1 is around 140 and in RICH 2 around 220 to be compared to $\sim 10$ in each of the RICH detectors in the absence of beam. Examination of the spatial distribution of the hits showed a concentration in the centre of the HPD. Owing to the configuration of the focusing electric field, this is characteristic of ion feedback within the HPD. Long-lifetime fluorescent states from the gas radiator would result in a uniform distribution over the HPD surface.

It was decided to quench the unwanted scintillation. This should be done with no significant loss of Cherenkov photons nor any appreciable change to the refractive index.

## 3. Scintillation in CF$_4$

Ultraviolet emission from excited CF$_4$ has been extensively studied [10]. Two separate emission systems are observed (Table 2 and Fig. 4). In Ref. [10], the relative scintillation photon yield is obtained with a rf-modulated beam of 200 V electrons passing through a low-pressure, 1.3 Pa, gas. The two emission systems appear continuous even at 0.04 nm resolution.

Photon emission data for wavelengths above 400 nm are available in Refs. [11,12] and further discussed in Ref. [13]. These data sets are given for gas pressures between 0.13 and 13 Pa. A bright yellow emission band is reported to lie in the region between 400 and 750 nm. This band has no structure. Collision-free UV band emission with lifetime in the 14–17 ns range is reported in Ref. [12]. The same lifetime range is given for the visible band emission. The origin of the VUV emission in CF$_4$ has been identified as due to transitions in CF$_4^+$ excited ions, while the UV and visible emissions originate in CF$_3$ excited molecules [14].

An absolute photon yield at 0.1 MPa gas pressure cannot easily be extracted from these low pressure, and thereby nearly collision-free, data sets as the shape and the strength of the different spectral bands might be modified. The yield is given in Ref. [15] for CF$_4$ gas pressures between 0.1 and 0.5 MPa. The data for a gas pressure of 0.2 MPa is shown in Fig. 5 together with the data from Ref. [10]. The two data sets agree well in the shape and relative strengths of the 9 ns lifetime emission system between 220 and 300 nm. The measurements from Ref. [15] for a gas pressure of 0.1 MPa give $\sim 2000 \pm 300$ photons/MeV between 200 and 500 nm and $\sim 700 \pm 150$ photons/MeV in the range 500–800 nm.

## 4. Quenching of CF$_4$ scintillation using radiationless transitions

The primary scintillation in our wavelength range is a cascade-free emission by the radical CF$_3$ as given in Table 2. This allows the possibility to quench the emission by radiationless transition [16,17] from the donor molecule to an acceptor molecule with a

**Table 2**
Radiative lifetimes ($\tau$) and wavelength ($\lambda$) of CF$_4$ emission systems in Ref. [10].

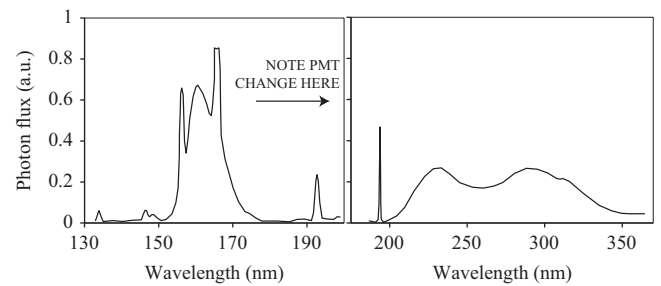| $\lambda$ (nm) | $\tau$ (ns) | Comment |
| --- | --- | --- |
| 160 | $2.1 \pm 0.2$ | Cascade free |
| 220–300 | 9.0 | Cascade free |



**Fig. 4.** The emission spectrum of CF$_4$ excited by 200 V electrons and recorded at 0.54 MHz modulation frequency. Data from Fig. 3 in Ref. [10].
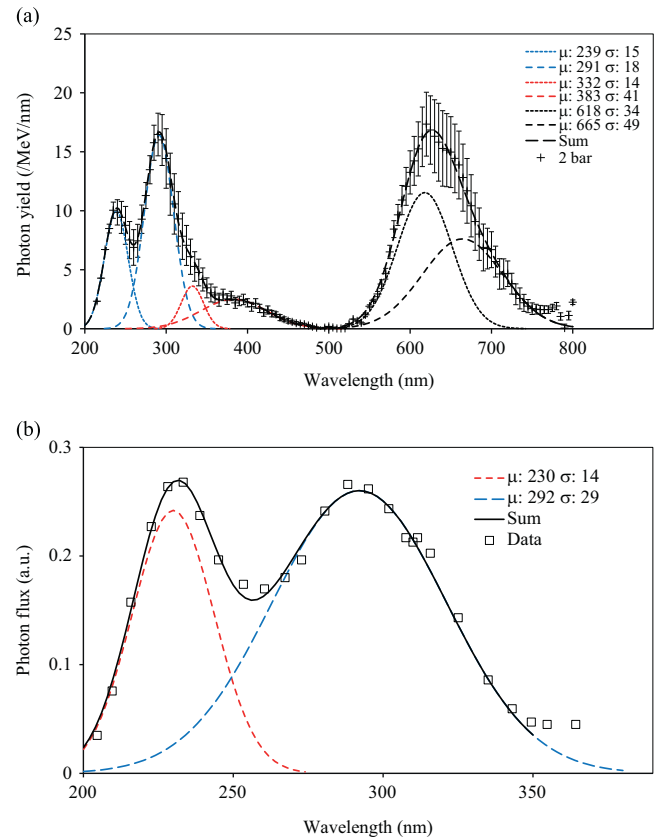


**Fig. 5.** (a) Scintillation photon yield between 200 and 800 nm in CF$_4$ at 0.2 MPa gas pressure. Only systematic uncertainties are shown (data from Ref. [15]). (b) Relative scintillation photon yield between 200 and 360 nm in CF$_4$ at a pressure of 1.3 Pa (data from Fig. 3 in Ref. [10]). Possible spectral bands are overlaid, parameterised as Gaussian with mean $\mu$ (nm) and standard deviation $\sigma$ (nm).

subsequent emission in the infrared. The classic study [18] of the problem obtained an equation relating the quenching of the fluorescence, $Q$, to the partial pressure of an added second gas:

$$Q = \frac{I}{I_0} = \frac{1}{1 + \tau_0 qC} \tag{1}$$

where $Q$, the quenching coefficient, is the ratio of fluorescence intensities with, $I$, and without, $I_0$, the second gas added. $\tau_0$ is the natural lifetime of the excited molecule, $q$ is the effective collision frequency and $C$ is the concentration by volume of the second gas.

Fig. 6 gives our measurements of the quenching coefficient for two gas mixtures, CF$_4$ with N$_2$ and CF$_4$ with CO$_2$. The gas, at room temperature and pressure, is excited by an Am$^{241}$ $\alpha$ emitter in the small test apparatus shown in Fig. 7. Photons are recorded with a Hybrid Photon Detector connected to an Analog to Digital

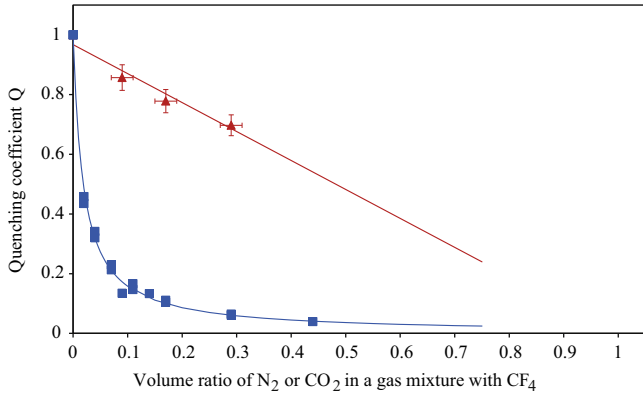**Fig. 6.** The quenching coefficient, Eq. (1), in $CF_4$ as function of volume concentration of $N_2$ (▲) and $CO_2$ (■) in the gas mixture.
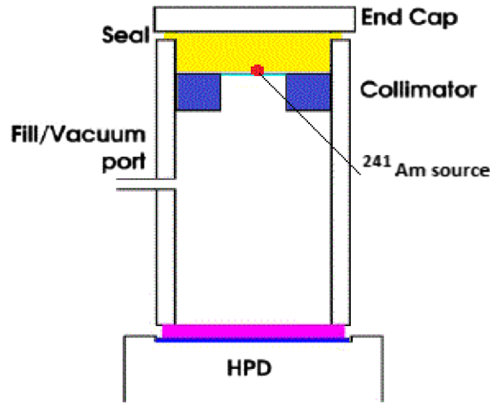


**Fig. 7.** Schematic diagram of the test cell used for the quenching measurements. The height of the cell is 54 mm and the diameter 24 mm.

Converter.[2] The photon detector is not sensitive below 200 nm. The intensities $I$, $I_0$ are measured using background-subtracted photon counting with the HPD. The admixture of $N_2$ to $CF_4$ has, as expected, no effect apart from diluting the gas. This is dramatically different with $CO_2$. A fit of our data to Eq. (1) gives $\tau_0 q = 53 \pm 2$ or $q = 5.9 \pm 0.6 \times 10^9$ s$^{-1}$ for the 9 ns lifetime system given in Table 2. If we assume ideal gases at 20 °C and 0.1013 MPa, a calculation of the mean speed and free path of the molecules gives a collision frequency in pure $CF_4$ and $CO_2$ as $6.6 \times 10^9$ s$^{-1}$ and $4.6 \times 10^9$ s$^{-1}$ respectively. Our measurement of $\tau q$ is valid only for wavelengths above 200 nm and cannot be used to assess the consequences for the 2.1 ns lifetime emission at 160 nm. However, the photon absorption coefficient in $CO_2$ at 160 nm [19] is $\sim 5$ cm$^{-1}$ bar$^{-1}$ corresponding to a length of about 2 cm with a 10% admixture by volume of $CO_2$ in $CF_4$.

The RICH 2 Cherenkov radiator was changed to $CF_4$ with about 5% admixture of $CO_2$. The refractive indices of $CF_4$ and $CO_2$ are given [20] as

$$(n-1)_{CF_4} = \frac{0.1249 \times 10^{-6}}{61.8^{-2} - \lambda^{-2}}$$

$$(n-1)_{CO_2} = \frac{0.0687 \times 10^{-6}}{80.1^{-2} - \lambda^{-2}}$$

in the standard one-pole Sellmeier approximation. The wavelength $\lambda$ is in nm and temperature and pressure are respectively 0 °C and 0.1013 MPa. Insertion of the limiting values for the wavelength

---

[2] ORTEC MODEL 926 ADCAM MULTICHANNEL BUFFER.

range of interest (200–800 nm) into the Sellmeier formula gives similar values for $n-1$ and for $\Delta n = n_{200} - n_{800}$. As a result the Cherenkov angle and hence also the Cherenkov photon yield are similar for $CF_4$ and for $CO_2$. Furthermore the chromatic dispersion, which determines the irreducible angular resolution, is similar. This admixture will therefore have only a minor impact on the performance of the RICH2 detector.

## 5. Quenching efficiency

Early in 2011 a mixture of $CF_4$ and a few percent $CO_2$ gas was injected into RICH 2. The $CO_2$ concentration has slowly varied by a few percentage points. The quenching effect can be seen in g?cFig. 8 by comparing to Fig. 1. The data in Fig. 8 were obtained at different instantaneous luminosity, $\mathcal{L}$, and the number of interactions per trigger, $\mu$, than those in Fig. 1. However, the effects from the different run conditions can be accounted for by assuming that RICH 1 and RICH 2 have unchanged detection efficiencies in 2011 as compared to 2010 and that the ratio of the charged particle density in the two detectors is unchanged. The effect of the admixture of $CO_2$ in $CF_4$ results, on the average, in a reduction of $\sim 25\%$ of recorded hits in RICH 2.

It has proven to be somewhat difficult to determine an observable for the quenching efficiency that is stable over time, insensitive to the trigger conditions and not too dependent on luminosity and the mean number of interactions per trigger. Some of the more obvious ones, such as the bias current of the silicon photo-electron detector in the HPD, are strongly correlated to environmental parameters like temperature and integrated particle flux. The most stable measurement has proven to be the number of hits recorded on the photon detector after removing large hit clusters originating from Cherenkov radiation or particle showers in the HPD entrance window. The data are given in Fig. 9. The data set includes all fills in 2011 where $200 \leq \mathcal{L} \leq 400 \times 10^{30}$ cm$^{-2}$ s$^{-1}$ and $1.3 \leq \mu \leq 1.6$.

The ratio of hits in RICH 2 and in RICH 1 is reasonably well described by a function $Z$ given as

$$Z = \frac{\text{RICH 2}_{hits}}{\text{RICH 1}_{hits}} = \frac{X \cdot (1 + A \cdot Q)}{B \cdot X} \quad (2)$$

where $X$ is the number of hits in RICH 2 if no scintillation is present, $A$ is the number of hits from scintillation photons for each Cherenkov photon hit, $B$ is a proportionality factor between RICH 1 and RICH 2 hits if no scintillation is present and $Q$ is the quenching coefficient given in Eq. (1). A fit to the data in Fig. 9 gives
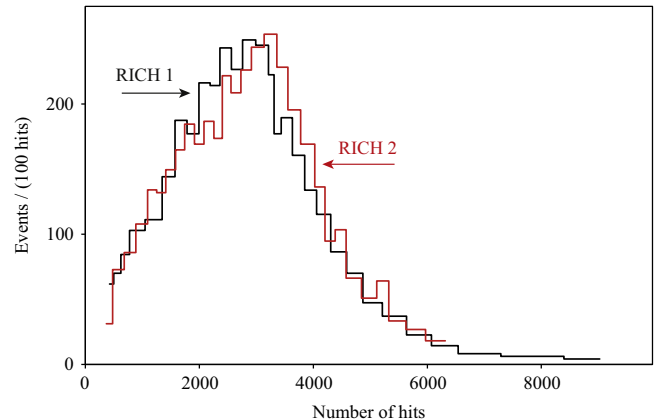
$A = 1.2 \pm 0.15$
$B = 1.16 \pm 0.04$



**Fig. 8.** RICH 1 and RICH 2 hits. Date: 20/03/2011, Fill: 1640, B: -1, Average $\mathcal{L}$ : $36.83 \times 10^{30}$ cm$^{-2}$s$^{-1}$, Average $\mu$: 1.93.
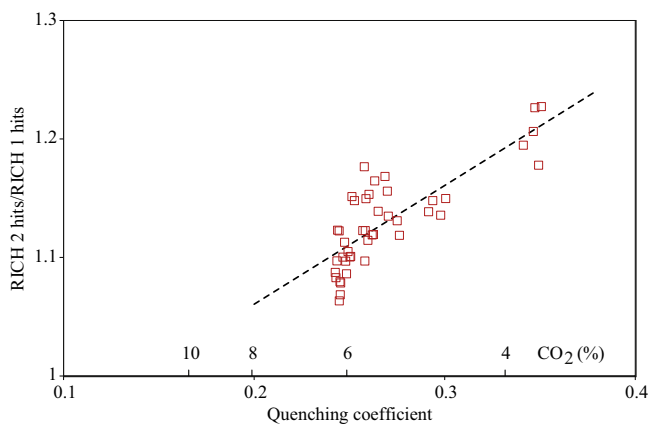
**Fig. 9.** The ratio between number of hits in RICH 2 to the number of hits in RICH 1 as a function of the quenching coefficient. Data from 2011.

for

$$Q = \frac{1}{1 + (53 \pm 2) \cdot C}$$

where all quoted uncertainties result from the fit. The value of 1.2, obtained for the parameter $A$, is in reasonable agreement with the ratio of gas scintillation to Cherenkov yield shown in Fig. 3. To validate this simple model we compare our data with expectations from simulation. However, the simulation does not include scintillation, while the data provide results for varying levels of quenching of the scintillation, which never reaches 100%. We therefore extrapolate $Z$ (using Eq. (2)) to the ideal case of no scintillation. This gives $Z \simeq 0.86 \pm 0.03$, if all scintillation in $CF_4$ would have been quenched, which can be compared to $Z = 0.67 \pm 0.01$, predicted by the simulation as given in Table 1. The number of hits in RICH 2 and in the detectors near to RICH 2 is about 25% less in simulation, as compared to data. We believe that this is due either to extra material in the real detector not accounted for in simulations or from the effects of "back-splash" from downstream detectors. This would account for the difference between the measured and the simulated values of $Z$.

## 6. Conclusion

We have shown that the scintillation photon emission of $CF_4$ in the UV to visible wavelength range can be efficiently quenched via the addition of a low concentration of $CO_2$, consistent with radiationless transitions to $CO_2$ with a subsequent emission in the infrared. This small admixture of $CO_2$ to $CF_4$ has an insignificant impact on the refractive index of the Cherenkov radiator.

## Acknowledgement

## References

[1] The LHCb Collaboration, Journal of Instrumentation 3 (2008) S08005 http://dx.doi.org/10.1088/1748-0221/3/08/S08005.
[2] The LHCb RICH Collaboration, The European Physical Journal C 73 (2013) 2431; The LHCb Collaboration, LHCb RICH Technical Design Report, CERN LHCC 2000-037, LHCb TDR 3, 6 September 2000.
[3] M. Moritz, et al., IEEE Transactions on Nuclear Science NS-51 (3) (2004) 1060; M. Alemi, et al., Nuclear Instruments and Methods in Physics Research Section A 442 (3) (2000) 164.
[4] A. Pansky, et al., Nuclear Instruments and Methods in Physics Research Section A 354 (1995) 262.
[5] See for example: R. Gernhäuser, et al., Nuclear Instruments and Methods in Physics Research Section A 371 (1995) 300; R. Pestotnik, Večanodna fotopomnoževalka kot krajevno občutljivi detektor Čerenkovih fotonov (Diploma thesis), Ljubliana, 1996; A. Kaboth, et al., Nuclear Instruments and Methods in Physics Research Section A 592 (2008) 63; and references therein.
[6] L. Tamburello, Misure di scintillazione nei radiatori del RICH di LHCb e studio di un canale di decadimento semileptonico per la calibrazione del Flavour Tagging, Tesi di Laurea Specialistica, Università Milano-Bicocca, 2009.
[7] R.W. Forty, O. Schneider, RICH pattern recognition, LHCb-98-040; R. Forty, Nuclear Instruments and Methods in Physics Research Section A 433 (1999) 257; R. Forty, Ring finding and particle identification, in: Landolt-Börnstein New Series, vol. I/21B1, 2011, p. 3.171.
[8] S. Easo, et al., IEEE Transactions on Nuclear Science NS-52 (1665) (2005).
[9] C. Barham, S. Katvars, S. Wotton, RICH L1 Technical Manual, CERN EDMS 768873, 16/08/2011.
[10] J.E. Hesser, K. Dressler, The Journal of Chemical Physics 47 (9) (1967) 3443.
[11] M. Suto, N. Washida, The Journal of Chemical Physics 78 (3) (1983) 1007.
[12] C.R. Quick Jr., et al., Chemical Physics Letters 114 (4) (1985) 371.
[13] T.Y. Jung, et al., Bulletin of the Korean Chemical Society 27 (3) (2006) 373.
[14] H.A. van Sprang, H.H. Brongersma, F.J. de Heer, Chemical Physics 35 (1) (1978) 51.
[15] A. Morozov, et al., Nuclear Instruments and Methods in Physics Research Section B 268 (2010) 1456.
[16] P. Seybold, M. Gouterman, Chemical Reviews 65 (4) (1965) 413.
[17] D.L. Andrews, Chemical Physics 135 (2) (1989) 195.
[18] O. Stern, M. Volmer, Physikalische Zeitschrift 20 (1919) 183.
[19] E. Albrecht, et al., Nuclear Instruments and Methods in Physics Research Section A 510 (2003) 262.
[20] R. Abjean, et al., Nuclear Instruments and Methods in Physics Research Section A 292 (1990) 593–594; H.E. Watson, K.L. Ramaswamy, Proceedings of the Royal Society of London A 156 (1936) 144; Landolt-Börnstein, Eigenschaften der Materie in hren Aggregatzuständen, 8, Teil, Optische Konstanten.